ELSEVIER

Available online at www.sciencedirect.com

ScienceDirect

Physics Procedia 2 (2009) 527–538

Physics Procedia

www.elsevier.com/locate/procedia

Anatase-to-rutile phase transition of samarium-doped TiO_2 powder detected via the luminescence of Sm^{3+}

Valter Kiisk[1*], Mari Šavel[1], Valter Reedo[1,2], Argo Lukner[1], Ilmo Sildos[1]

[1] *Institute of Physics, University of Tartu, Riia Str. 142, 51014 Tartu, Estonia*

[2] *Institute of Organic and Bioorganic Chemistry, University of Tartu, Jacobi Str. 2, 51014 Tartu, Estonia*

Abstract

We employed a sol-gel route to prepare 1% samarium-doped TiO_2 nanopowders. Time-resolved photoluminescence (PL) and Raman characterization was performed. After a thermal treatment the powder crystallized in an anatase phase and revealed intense Sm^{3+} photoluminescence. The emission spectrum of Sm^{3+} exposed well-resolved crystal-field splitting enabling monitoring of the changes in the local environment.

We thoroughly investigated the influence of the annealing treatment (in air) on Sm emission intensity. Annealing up to 800°C led to a systematic enhancement of Sm emission. Annealing at higher temperatures, however, led to a marked weakening of Sm^{3+} emission and simultaneous appearance of an emission band near 830 nm. Annealing temperatures as high as 1000°C were needed to induce the phase transition from anatase to rutile. It was possible to use Sm^{3+} as a structural probe revealing peculiarities of the phase transition.

PACS: 78.55.Hx, 78.47.Cd, 78.67.Bf, 81.20.Ev

Keywords: titanium dioxide, rare earths, photoluminescence, sol-gel method, sintering.

[*] Corresponding author. Institute of Physics, University of Tartu, Riia Str. 142, 51014 Tartu, Estonia. Tel.: +372-7374613; fax: +372-7383033; e-mail: kiisk@ut.ee

doi:10.1016/j.phpro.2009.07.038

1. Introduction

Titanium dioxide (TiO_2) appears to be a promising wide-gap (3.2 eV) semiconductor for rare earth (RE) activation [1,2,3]. The possibility of carrier-mediated RE excitation suggests an application potential in injection devices and in phosphors requiring near-UV photoexcitation (e.g. LED phosphors). The high refractive index of TiO_2 facilitates its use in integrated photonics [4].

Sol-gel preparation method is preferentially employed for preparation of metal oxides due to its morphological flexibility, low operation temperature and easy inclusion of impurities. Most sol-gel routes lead to TiO_2 powder or thin film in anatase phase due to the nanocrystalline nature of the material obtained. Much work is required to optimize the preparation in favour of RE emission considering phase stability, size of nanocrystals, impurity content, annealing conditions and surface passivation. The latter is especially important as RE emission in TiO_2 exhibits a marked sensitivity to the ambient [5].

The main goal of the present work was to perform a systematic study of the luminescent and structural behavior of Sm-doped TiO_2 powder as a function of annealing treatment. Due to their sharp emission lines the Sm^{3+} ions could also be used as a luminescent probe reflecting the peculiarities of the anatase-to-rutile phase transition. In addition, special attention has been devoted to the study of Sm^{3+}:TiO_2 emission under direct excitation as so far most reports have been dealing with host-sensitized emission.

2. Samples and experimental

A sol-gel route based on hydrolysis and polycondensation of $Ti(OBu)_4$ was employed for preparation of Sm-doped TiO_2 nanocrystalline powder where the nominal molar ratio of Sm^{3+}/Ti^{4+} was 1 at%. First, a solution containing 0.04 g $SmCl_3 \cdot 6H_2O$ (Alfa Aesar, 99.9%), 0.041 g concentrated HCl (AppliChem), 3.756 g hexane and 0.166 g dist. water was prepared. 0.512 g of this solution was mixed into another solution containing 0.01 g of $C_2H_5NHC_2H_5$ in 3.488 g of hexane. About 6 g of distilled n-buthanol (YA-KEMIA OY) was added to capture Sm. After about an hour of sedimentation the salt H_5C_2-NCl-C_2H_5 was filtered out. The solvent was removed in rotator evaporator at 4 mmHg. The

remaining 0.345 g of substance was mixed into a solution containing ~4 g of $Ti(OBu)_4$ (Alfa Aesar, 98+%) in 5.334 g of hexane. The solution was drop-wise added into stirred dist. water at 75°C. Powder was formed by drying the colloidal solution at 100°C in vacuum.

It should be mentioned that properly modified procedure allowed also preparation of free-standing films and waveguiding fibers with nearly identical luminescent properties (not to be discussed here).

For excitation of the luminescence a 150 W Hamamatsu xenon source was used in combination with a monochromator (MDR-23, spectral width 2 nm). For time-resolved measurements an OPO light source from Expla Ltd (pulse width 3 ns, pulse energy ~50 μJ, repetition rate 20 Hz) was employed. The spectra were recorded by using a spectrograph (Andor SR-303i) equipped with an image-intensified charge coupled device (Andor DH-501) permitting time-resolution down to 5 ns. All measurements were performed at room temperature. Spectra were corrected to instrumental response.

The Raman spectra were recorded in a backscattering geometry by using a homemade micro-Raman spectrometer consisting of a confocal microscope with 50x objective, a Nd^{3+}:YAG laser operating at 532 nm, a notch filter for removal of the scattered laser light, and Andor SR-303i spectrograph equipped with an EMCCD detector (estimated spectral resolution 1.5 cm^{-1}).

During the PL measurements as well as heat treatments the powder was placed into a high-quality quartz cuvette. The samples were repeatedly annealed in air by insertion into a pre-heated furnace.

3. Results and discussion

The initial dried samples were amorphous according to Raman spectrum (Fig. 1) and exposed no sign of Sm emission. The anatase phase as well as intense Sm^{3+} emission under a band-to-band excitation (355 nm) of the TiO_2 host started to emerge after annealing at 350–400°C (corresponding apparently to the release of carbon of organic residues, considering the blackening of the material at lower-temperature heat treatments). XRD-analysis (data not shown) performed on the sample annealed

at 600°C indicates pure anatase phase and a crystallite size of 12 nm (calculated from the XRD spectrum line broadening using the Scherrer equation).

The PL spectrum (Fig. 2) has a well-established fine structure indicating that Sm^{3+} ions are fitted into well-defined positions in the crystal lattice. The excitation spectrum is prevailed by an intense broad excitation band at photon energies exceeding the band-gap of anatase (3.2 eV) and attributed to the host-sensitization of Sm^{3+}. Weak features at 410 and 475 nm are due to the direct excitation of Sm^{3+}.

The host-sensitized Sm^{3+} PL spectrum appears identical to that of anatase TiO_2 crystalline films prepared by using an entirely different approach [2,8] and can be considered as a spectral "fingerprint" of Sm^{3+} in the anatase phase of TiO_2. However, under direct excitation of Sm^{3+} some additional spectral lines were noticed that were not observable under 355 nm excitation (Fig. 3). The lines were more pronounced in the case of low-temperature annealing. Similar spectrum under 488 nm excitation was reported by Bettinelli et al [9]. Time-resolved spectra (same figure) indicate that these additional features indeed have somewhat different decay kinetics. They can be grouped into two sets where the spectral lines within each set have the same decay rates. Similar grouping was possible for spectra corresponding to different annealing (not shown) only the relative importance of the different sets would be different. This suggests that there exists three major Sm^{3+}-related emission centers in anatase TiO_2 whereas only one of them is involved in the energy transfer from host to guest. The existence of several Sm^{3+} emission centers is natural due to the requirements of local charge compensation suggesting the presence of a charged defect (probably an oxygen vacancy) in the vicinity of RE ion [10].

Decay kinetics measured around 612 nm displays at least double-exponential behavior as expected (Fig. 4). It appears that the lifetime of the emission from the "regular" sites (that are observable under host-sensitized excitation) is about 285 μs.

Systematic investigation of the influence of annealing treatment on TiO_2:Sm powders was performed. It turns out to be that the host-sensitized PL intensity saturates about in an hour when

annealed at a fixed temperature (Fig. 5). Subsequent increase of annealing temperature leads to a similar increasing of PL intensity. Such process could be repeated till 800°C, which appears to be the optimum heat treatment for this material. Such behavior suggests that multiple stages of recovery with different activation barriers are present. At low annealing temperatures the behavior is most probably connected to the release of organic traces and densification of the material. In addition, growth of crystallites, release of adsorbed OH species and elimination of defects in the crystal lattice may contribute to the increasing PL intensity. The crystal growth is typically reflected in the systematic narrowing of Raman lines of anatase as also observed in the present case (Fig. 6). Comparison of the width of the 144 cm^{-1} Raman line to the data of Ref. 11 reveals an increase of the crystallite size from 7 to 15 nm. The essential role of hydroxyl groups has been identified in the case of TiO_2:Er^{3+} by using FTIR [12]. At highest annealing temperatures defect relaxation processes analogous to those in ion-implanted materials might be essential [13].

We also observed that the intensity of the PL emission of optimally annealed powder decreased several times if the sample was kept a couple of days in ambient conditions. In addition, a marked shift in the excitation spectrum was noticed. Subsequent heating to 200°C restored the initial intensity. This indicates that the emission of the nanopowder is fairly sensitive to surface contamination (humidity) and some surface capping might be necessary for practical application of such material.

Further annealing treatments (at 900°C and up) led to a gradual weakening of Sm^{3+} emission and simultaneous appearance of a near-infrared emission band centered at ~830 nm (Fig. 7). Similar infrared emission has been frequently noticed in both anatase and rutile phases [14,15] and has been ascribed to Ti^{3+} defects [16] formed as the result of the formation of oxygen vacancies due to the loss of oxygen during high-temperature annealing. Some authors relate the emission more directly to the (ionized) oxygen vacancies [17]. The formation of oxygen vacancies could be avoided only through the use of high-pressure atmosphere during the heating [18]. It is somewhat complicated to identify the main reason of Sm^{3+} PL quenching as several changes take place nearly simultaneously at 900–1000°C: anatase-to-rutile phase transition [19], migration of RE ions onto surface [20,21], and

formation of Ti^{3+} defect centers which is believed to serve as concurrent radiative relaxation channels [15]. However, the results of the present experiment seem to suggest that quenching of Sm emission is initiated before the phase transition as Sm^{3+} fine structure indicates no changes before annealing at 1000°C. Furthermore, Fig. 7 suggests that there is an interplay between the Sm^{3+}- and Ti^{3+}-related emission intensities supporting the essential role of Ti^{3+} defects as also proposed in the case of Eu emission in TiO_2 [15].

According to Raman spectra (Fig. 8) nearly 1000°C is needed to initiate anatase-to-rutile phase transition. From the ratio of the 395 cm^{-1} anatase band and the 445 cm^{-1} rutile band it is possible to estimate [22] that after 5 min of heat treatment at 1000°C already 80% of the material is in rutile phase. Indeed, the Sm^{3+} emission excited by 477 nm reveals a complete modification of the fine structure (Fig. 9). However, the host-sensitized Sm^{3+} emission retains the fine structure typical of an anatase phase. A prolonged heat treatment of more than 15 min was required to induce a similar change of Sm^{3+} spectrum under 355 nm excitation. The result can be explained by taking into account that the penetration depth for 355 nm radiation is of the order of only 200 nm in TiO_2 (according to absorption data in Ref. [23]). Therefore the directly excited Sm^{3+} emission characterizes the bulk of the material whereas host-sensitized emission originates from the ions near the surface of an agglomerated powder particle. Therefore we conclude that the rutile phase forms initially in the interior of powder particles and subsequently propagates to the surface. It is in accordance to a previously published UV-Raman study [22]. It has been proposed that the phase transition is initiated at the interfaces of contacting anatase crystallites of agglomerated TiO_2 particles.

Anatase-to-rutile phase transition is typically complete already at ~700°C in pure bulk materials [22]. However, the nanocrystallinity as well as the nature of impurities can markedly influence the transition temperature in a quite complicated manner [24,25]. In the present case it is most probable that the rare earth impurities inhibit the growth of nanocrystallites, which, in turn, stabilizes the anatase phase [19].

4. Conclusions

It is concluded that crystallite growth, release of OH species and defect relaxation in sol-gel-derived TiO_2:Sm nanopowders leads to the enhancement of Sm^{3+} emission up to the annealing temperature of 800°C whereas higher temperatures introduce Ti^{3+} defects which might be responsible for the quenching the emission of Sm^{3+} ions.

Three different Sm^{3+}-related emission centers seem to exist in anatase TiO_2 whereas only one of them is subject to the energy transfer from host to guest.

Most remarkably, Sm^{3+} ion proves to be a good structural probe in TiO_2 providing supporting evidence that during an anatase-to-rutile phase transition the rutile phase is initially formed in the interior of an agglomerated powder particle and subsequently propagates to the surface. The spectrum of Sm^{3+} in the rutile phase of TiO_2 (being markedly different from that in the anatase phase) is reported for the first time.

5. Acknowledgements

The authors are grateful to Hugo Mändar for conducting XRD analysis and to Martti Pärs for the installation of the Raman setup and useful discussions regarding TiO_2 Raman characterization. Estonian Science Foundation is acknowledged for financial support (grants nos. 7456, 6999 and 6660).

6. References

[1] K.L. Frindell, M.H. Bartl, M.R. Robinson, G.C. Bazan, A. Popitsch, and G.D. Stucky, J. Solid State Chem. 172 (2003) 81.

[2] S. Lange, I. Sildos, V. Kiisk, and J. Aarik, Mat. Sci. Eng. B 112 (2004) 87.

[3] 1.C. Gao, et al., J. Lumin. 128 (2008), 559–564.

[4] A. Chiasera et al, Optical Materials 25 (2004) 117.

[5] V. Reedo, S. Lange, V. Kiisk, A. Lukner, T. Tätte, and I. Sildos, Proc. SPIE 5946 (2005) 59460F.

[6] T.D. Robert, L.D. Laude, V.M. Geskin, R. Lazzaroni, and R. Gouttebaron, Thin Solid Films 440 (2003), 268–277.

[7] F.S. Liu, et al., J. Lumin. 111 (2005), 61–68.

[8] V. Kiisk, I. Sildos, S. Lange, V. Reedo, T. Tätte, M. Kirm, and J. Aarik, Appl. Surf. Sci. 247 (2005) 412.

[9] M. Bettinelli, A. Speghini, D. Falcomer, M. Daldosso, V. Dallacasa, and L. Roman, J. Phys. Cond. Matt. 18 (2006) S2149.

[10] D.F. Crabtree, J. Phys. D. 11 (1978), 1543–1551.

[11] S. Kelly, F.H. Pollak, and M. Tomkiewicz, J. Phys. Chem. B 101 (1997) 2730–2734.

[12] A. Bahtat, M.C. Marco de Lucas, B. Jacquier, B. Varrel, M. Bouazaoui, and J. Mugnier, Opt. Mat. 7 (1997) 173.

[13] E. Alves, J.V. Pinto, R.C. da Silva, M. Peres, M.J. Soares, and T. Monteiro, Nucl. Instr. Meth. B. 250 (2006), 363–367.

[14] R. Plugaru, A. Cremades, and J. Piqueras, J. Phys. Cond. Matt. 16 (2004) S261.

[15] C.W. Jia, E.Q. Xie, J.G. Zhao, Z.W. Sun, and A.H. Peng, J. Appl. Phys. 100 (2006) 023529.

[16] A.K. Ghosh, F.G. Wakim, and R.R. Addiss, Phys. Rev. 184 (1969) 979.

[17] 1.F. Montoncello, et al., J. Appl. Phys. 94 (2003), 1501–1505.

[18] T. Sekiya, K. Ichimura, M. Igarashi, and S. Kurita, J. Phys. Chem. Solids 61 (2000) 1237.

[19] E. Setiawati and K. Kawano, J. Alloys & Comp. 451 (2008) 293–296.

[20] L.A. Rocha, L.R. Avila, B.L. Caetano, E.F. Molina, H.C. Sacco, K.J. Ciuffi, P.S. Calefi, and E.J. Nassar, Materials Research 8 (2005), 361–364.

[21] E. Setiawati, K. Kawano, T. Tsuboi, H.J. Seo, Jap. J. Appl. Phys. 47 (2008), 4651–4657.

[22] J. Zhang, M. Li, Z. Feng, J. Chen, and C. Li, J. Phys. Chem. B 110 (2006) 927.

[23] H. Tang, K. Prasad, R. Sanjines, P.E. Schmid, and F. Lévy, J. Appl. Phys. 75 (1994) 2042.

[24] D.J. Reidy, J.D. Holmes, M.A. Morris, J. Eur. Ceram. Soc. 26 (2006) 1527.

[25] R. D. Shannon and J. A. Pask, J. Am. Ceram. Soc.48 (1965) 391.

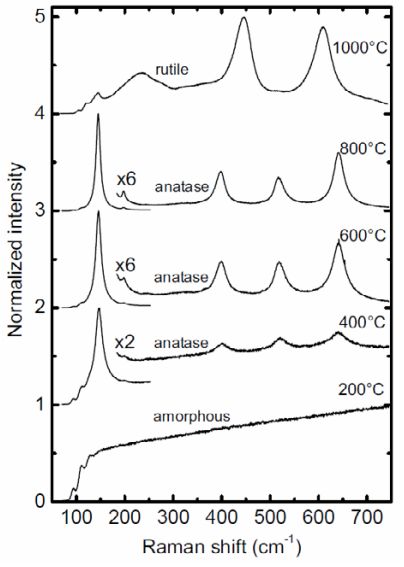

Fig. 1. The Raman spectra of sol-gel-derived TiO_2:Sm powder after annealing treatments at different temperatures. Assignment of phases is according to Ref. 6.

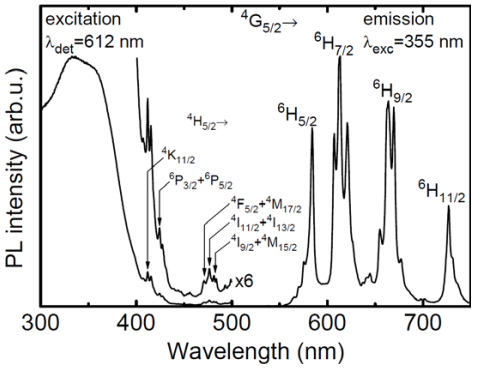

Fig. 2. The luminescence and its excitation spectrum of sol-gel-derived TiO_2:Sm powder annealed at 600°C. The part of the excitation spectrum corresponding to direct excitation of Sm^{3+} has been amplified for clarity. The transitions of direct excitation have been assigned according to Ref. 7.

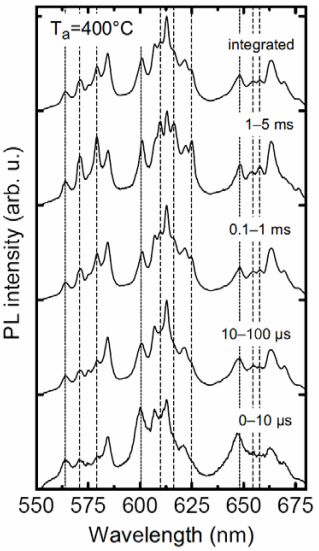

Fig. 3. Time-resolved PL spectrum of TiO_2:Sm^{3+} powder (annealed at 400°C) excited at 477 nm. Dashed and dotted lines group the spectral lines of similar decay kinetics. Note that all spectra are normalized and only the ratio of the intensities of different features should be considered.

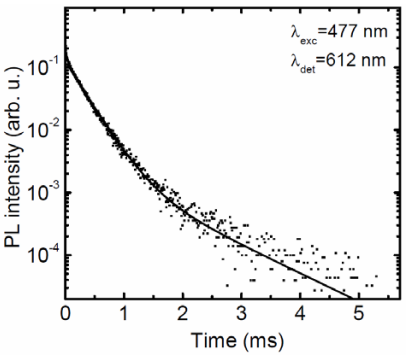

Fig. 4. Decay kinetics of PL of TiO_2:Sm powder (annealed at 800°C) measured at 612 nm with the spectral window of 2 nm. The decay is fitted by double-exponential with decay times 285 and 960 µs.

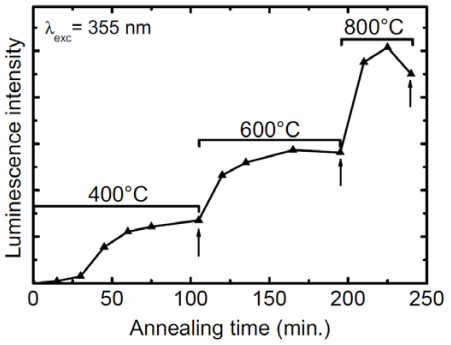

Fig. 5. Evolution of host-sensitized Sm^{3+} emission intensity of TiO_2:Sm powder as a function of annealing time and temperature. The abscissa axis represents the total (accumulating) annealing time over all temperatures. The arrows indicate the states where Raman spectra have been recorded.

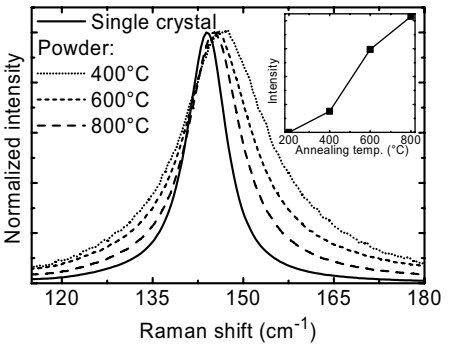

Fig. 6. The normalized 144 cm^{-1} Raman line of anatase powder after different annealing treatments. For comparison, the corresponding Raman line of a single-crystal anatase has been included. The inset displays the evolution of Raman intensity.

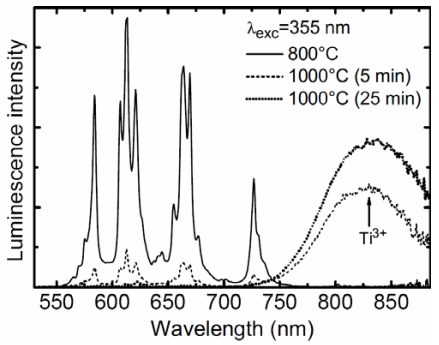

Fig. 7. The evolution of the PL spectrum of TiO_2:Sm powder after annealing at high temperatures.

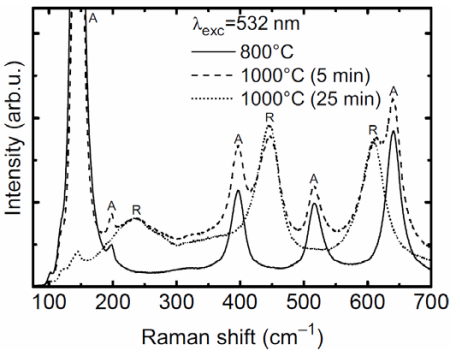

Fig. 8. The evolution of the Raman spectrum of TiO_2:Sm powder after annealing at high temperatures. Raman peaks due to anatase and rutile are indicated by letters A and R, respectively.

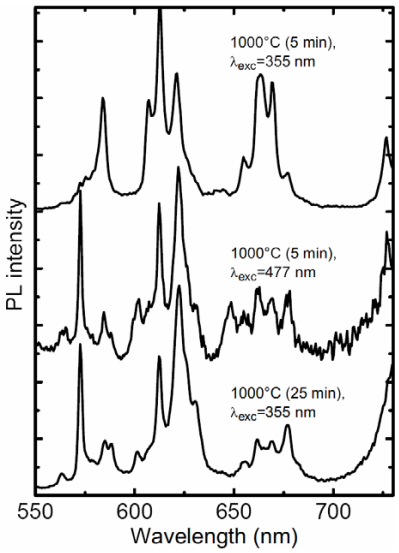

Fig. 9. Comparison of the host-mediated and the directly excited PL spectra of TiO_2:Sm^{3+} powder annealed at 1000°C.